Intrinsic lineshape of Josephson radiation from layered superconductors

L. N. Bulaevskii, I. Martin, and Gábor B. Halász
Los Alamos National Laboratory, Los Alamos, New Mexico 87545, USA
(Received 12 April 2011; published 26 July 2011)

We consider the radiation from the BSCCO crystal, which is long in the c-axis (z) and b-axis (y) directions but short in the a-axis (x) direction, so that $L_x \ll \lambda_\omega$, $L_y > \lambda_\omega$, and $L_z < \lambda_\omega/2$, where L_x, L_y, L_z are the crystal lengths along the x,y,z directions, respectively, while $\lambda_\omega = 2\pi c/\omega_J$ is the radiation wavelength and ω_J is the Josephson frequency. Metallic screens with lengths bigger than λ_ω are attached to the edges $\pm L_z/2$ to separate the half-spaces $|x| > L_x/2$ and inject a dc interlayer current into the crystal. This bias current induces the Josephson oscillations with frequency ω_J, which depends on the current. The oscillations result in the radiation from crystal edges $x = \pm L_x/2$. Such a radiation has a backward effect on the Josephson oscillations and, as a result, the total radiation power $\mathcal{P}_{\rm rad}$ depends on the geometrical factor $a = \epsilon_c L_x/L_z$ (ϵ_c is the dielectric constant of crystal for the electric field along the $c$axis) so that $\mathcal{P}_{\rm rad}$ is proportional to the number of junctions squared only when $a \gtrsim 1$. We show that both the super-radiation and the shunt capacitance attached to the screens introduce coupling of each junction with all others in the stack and, thus, stabilize the synchronized Josephson oscillations in all intrinsic junctions by forming the gap in the spectrum of fluctuation mode with nonzero momenta. To derive the linewidth of radiation, we account for pair-current fluctuations as well as fluctuations caused by quasiparticle currents. The gapless fluctuation mode with zero momentum related to the degeneracy with respect to the overall phase results in the broadening of the radiation line inversely proportional to the crystal volume. We estimate that the relative linewidth at 1 THz may be as narrow as 10^{-8} in the crystal with $L_y = 300$ μm. The fluctuations with nonzero momenta result in the suppression of the radiation power characterized by the parameter similar to the Debye-Waller factor.

DOI: 10.1103/PhysRevB.84.014516 PACS number(s): 85.25.Cp

I. INTRODUCTION

The possible use of Josephson junctions (JJs) as a source of electromagnetic radiation was discussed just after prediction of the ac Josephson effect. However, an emittance from a single JJ turns out to be very weak (of the order $\sim 10^{-6}$ μW) due to the small size of the radiating area (effective junction thickness) in comparison with the radiation wavelength.[1] Since then, JJ arrays were used as a source of coherent radiation[2,3] with the goal to achieve high radiation power proportional to the square number of junctions in an array. In this way, the radiation power of the order 10 μW was observed at discrete frequencies below 0.4 THz from an array of 500 junctions.[4] An important factor complicating synchronization of large numbers of artificial junctions is that it is only possible to fit a limited number of them into the region smaller than the radiation wavelength and so they have to be distributed over larger distances.[2,3] Nevertheless, synchronization of 7500 niobium junctions has been recently reported generating 2 μW of electromagnetic-wave power at a frequency of 76 GHz.[5] On the other hand, superconductors composed of layers connected by the intrinsic Josephson junctions with atomic effective thickness provide the possibility to have up to 10^5 JJ on the wavelength scale.[6]

THz radiation from intrinsic Josephson junctions (IJJ) was observed recently by use of small $Bi_2Sr_2CaCu_2O_{8+\delta}$ mesas biased with dc current along the c axis.[7] In this case, crystal works as a cavity to excite particular Fiske resonances determined by the geometry, while part of the electromagnetic field stored inside the mesa leaks outside of the crystal as a radiation. The radiation power was found to be proportional to a squared number of junctions N in the mesa, i.e., the super-radiation regime was achieved. As N was not very large, about 600, the radiation power was of the order μW. Such a device is not tunable with respect to frequency as resonance frequency is fixed by the mesa geometry.

The alternative design that provides a tunability was proposed in Ref. 8. It uses a crystal long in b (y axis) and c axes (z axis). The size of the crystal in the y direction L_y is supposed to be larger than the wavelength of radiation $L_y > \lambda_\omega = 2\pi c/\omega_J$, where ω_J is the radiation frequency (Josephson frequency). The size in the z direction is supposed to be smaller than $\lambda_\omega/2$ so that all junctions may be in phase with the radiation field. Under this condition, the number of junctions $N = L_z/s$ does not exceed 10^5. Here, s is the interlayer distance, 15.6 Å. The length L_x along the a axis should not be large to avoid excitations of the Fiske resonances in this direction and also to diminish heating. The bias dc current I induces voltage between layers V due to quasiparticle dissipation. This voltage causes the Josephson oscillations with the frequency $\omega_J = 2eV/\hbar$. Alternating electric E_z and magnetic B_y fields result in the radiation outside of the crystal in the x direction with the power $P \propto N^2 L_y$ at $\epsilon_c L_x \gtrsim L_z$ (ϵ_c is the high-frequency dielectric constant of the crystal). It may reach a value P/L_y as high as 0.5 W/cm in crystal with $L_x = 10$ μm and $L_z = 160$ μm.

The proposed design is shown in Fig. 1. It includes crystal, metallic screens at $|z| > L_z/2$ with a length larger than λ_ω in the z direction to eliminate destruction interference of waves radiated from the crystal edges $x = \pm L_x/2$, while the crystal itself with $L_y > \lambda_\omega$ screens such waves in the y direction. A shunt capacitor with the capacitance C_s is attached to the metallic screens to stabilize synchronized Josephson oscillations in different junctions.[9,10]

Here, we calculate the radiation linewidth from the system shown in Fig. 1 accounting for quasiparticle-current fluctuations and fluctuations of the pair current.[11,12] In the

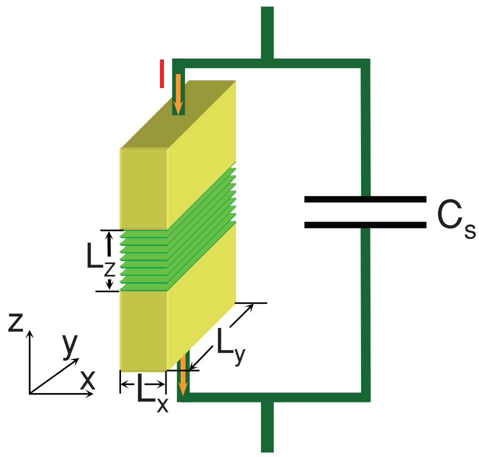

FIG. 1. (Color online) Stack of intrinsic Josephson junctions shunted by an external capacitance. Light yellow plates are metallic screens to eliminate destructive interference of electromagnetic waves emitted from the right and the left sides of the crystal, while the crystal itself (dark green) with $L_y > \lambda_\omega$ screens such waves in the y direction. Superconducting layers are shown by dark green.

super-radiation regime at $L_z \leqslant \epsilon_c L_x$, when the radiation power is proportional to N^2, one anticipates very narrow linewidth in analogy with that in lasers, where it is inversely proportional to the number of excited atoms in the working cavity.[13] Indeed, we show that the width of the central radiation line is inversely proportional to the crystal volume.

This paper is organized as follows. In the next section, we present the Lagrangian approach to find equations for the phases of superconducting order parameter and for the electromagnetic fields accounting for the shunt capacitor. In Sec. III, we write down boundary conditions for phase difference equations and find a solution for the phase differences and fields without accounting for fluctuations. In Sec. IV, we derive the amplitudes and frequencies of fluctuating modes. In Sec. V, we find the correlation function of Josephson oscillations accounting for fluctuations, which allows us to derive the radiation linewidth.

II. THE LAGRANGIAN AND EQUATIONS FOR PHASES AND FIELDS

The equations for phase differences and fields and corresponding boundary conditions for a radiating stack of IJJ were presented in Ref. 8. In this paper, we account additionally for the shunt capacitance and fluctuation currents. Chernikov and Schmidt[9] discussed the effect of a shunt in a stack of pointlike junctions and found that the capacitance shunt stabilizes synchronized Josephson oscillations in different junctions. For this, they used Josephson equations with external current in the right-hand side of these equations and accounted for current splitting between the stack and the shunt. This approach to account for a shunt does not work for extended junctions that we consider here because interlayer currents are nonuniform in the x,y plane inside the layers in the presence of radiation and of fluctuation currents. Thus, we use the Lagrangian approach[14] to treat the phases and the fields inside the crystal as well as the shunt. This allows us to conveniently account for a shunt as the total Lagrangian of the system with a shunt is simply the sum of that without a shunt and the shunt Lagrangian.

The Lagrangian for the system with a shunt shown in Fig. 1 is

$$\mathcal{L}\{\phi_n,\mathbf{A}\} = \epsilon_0 \sum_n \int d\mathbf{r}\Big[\frac{1}{2c_0^2}\dot{\varphi}_n\big(1-\alpha\nabla_n^2\big)^{-1}\dot{\varphi}_n - \frac{1}{\lambda_J^2}(1-\cos\varphi_n) - \mathbf{Q}_n^2\Big] - \int d\mathbf{r}\,dz\frac{(\nabla\times\mathbf{A})^2}{8\pi} + \frac{\hbar^2}{8e^2}C_s N^2\dot{\varphi}^2, \quad \epsilon_0 = \frac{\Phi_0^2 s}{16\pi^3\lambda_{ab}^2}, \tag{1}$$

$$\varphi_n = \phi_n - \phi_{n+1} - \frac{2\pi}{\Phi_0}\int_{ns}^{(n+1)s} dz\, A_z. \tag{2}$$

Here, $\varphi_n(\mathbf{r},t)$ is the gauge-invariant phase difference between the layers n and $n+1$, the coordinates inside layer are $\mathbf{r} = x,y$, the London penetration lengths are λ_c and λ_{ab} for currents between layers and inside layers, respectively, ϵ_c and ϵ_{ab} are the high-frequency dielectric constants for electric fields perpendicular to layers (along the z axis) and along the layers $\ell = \lambda_{ab}/s$. Further, $c_0 = c/(\sqrt{\epsilon_c}\ell)$, $\lambda_J = \gamma s$ is the Josephson length, $\gamma = \lambda_c/\lambda_{ab}$ is the anisotropy ratio, and $\Phi_0 = \pi\hbar c/e$. The first term accounts for the capacitance in the junctions n and change of the chemical potential μ_n in the layer n. The factor $(1-\alpha\nabla_n^2)^{-1}$, with second discrete derivative $\nabla_n^2 A_n = A_{n+1} + A_{n-1} - 2A_n$ and $\alpha = (4\pi e^2 s^2)^{-1}\partial\mu/\partial\rho = \hbar^2/(4e^2 s m^*)$, accounts for the relation between the gauge-invariant time derivative of the phase difference and the difference in the electrochemical potential (see Ref. 15):

$$\hbar\frac{\partial\varphi_n}{\partial t} = -esE_{zn} + \frac{\partial\mu}{\partial\rho}(\rho_n - \rho_{n+1}), \tag{3}$$

where m^* is the electron effective mass in the CuO_2 layers, V_n, $\rho_n(\mathbf{r}) = (E_{z,n+1} - E_{z,n})/(4\pi s)$, and $\mathbf{E}_n$ are the potential, the charge density, and the electric field in the layer n. Equation (3) results in the relation connecting the electric field inside the junction between the layers $n+1$ and n with the time derivative of the phase difference

$$E_{zn}(\mathbf{r},t) = \big(1-\alpha\nabla_n^2\big)^{-1}(B_c\lambda_c\ell/c)\dot{\varphi}_n(\mathbf{r},t), \quad B_c = \Phi_0/(2\pi\lambda_{ab}\lambda_c). \tag{4}$$

Taking $s = 15.6$ Å and $m^* = 5m_e$, we estimate $\alpha = 0.001$. Thus, we ignore charge coupling of layers in the following. The sum of the energy of the electric field $E_{zn}^2/(8\pi)$ and that accounting for the change of the chemical potential in the junction n, i.e., $\alpha\rho_n^2/2$, is the first term in the square brackets of Eq. (1). The second term is the Josephson coupling in the junction n. The third term in the square brackets describes the intralayer currents inside the crystal. In this term, $\mathbf{Q}_n = -\nabla\phi_n - (2\pi/\Phi_0)\mathbf{A}_n$ and ϕ_n is the phase of the superconducting order parameter in the layer n, while $\mathbf{A}_n(\mathbf{r})$ is the vector potential in the layer n. The intralayer current is $\mathbf{j}_n = (c\Phi_0/8\pi^2\lambda_{ab}^2)\mathbf{Q}_n$. We omit here the kinetic intralayer terms containing $\dot{\mathbf{Q}}_n$ because they are important at high frequencies of the order of intralayer plasma frequencies only, while at low frequencies, they have additional small parameter γ^{-2} in comparison with the first term. The next term in the Lagrangian is the energy of the electromagnetic field inside the crystal. The shunt capacitor is accounted for by the last term with the capacitance C_s, and here we introduced the average phase difference

$$\varphi(t) = \frac{1}{N}\sum_n \int \frac{d\mathbf{r}}{L_x L_y}\varphi_n(\mathbf{r},t). \quad (5)$$

The additional term in the Lagrangian due to the shunt is $\mathcal{L}_s = (\hbar^2/8e^2)C_s N^2\dot{\varphi}^2$. The shunt capacitor effectively enhances the capacitance of Josephson junctions but, only for synchronized oscillations, this enhancement is proportional to the number of junctions. This term introduces the coupling of each junction in the stack with all others.

We account for dissipation caused by the quasiparticle by introducing the dissipative function $\mathcal{R}\{\phi_n,\mathbf{A}\} = \mathcal{R}_c\{\phi_n,\mathbf{A}\} + \mathcal{R}_{ab}\{\phi_n,\mathbf{A}\}$, where

$$\mathcal{R}_c\{\phi_n,\mathbf{A}\} = \epsilon_0 \sum_n \int d\mathbf{r}\frac{2\pi\sigma_c}{c_0^2\epsilon_c}\dot{\varphi}_n^2, \quad (6)$$

$$\mathcal{R}_{ab}\{\phi_n,\mathbf{A}\} = \epsilon_0 s^2 \sum_n \int d\mathbf{r}\frac{2\pi\sigma_{ab}}{c_0^2\epsilon_{ab}}\dot{\mathbf{Q}}_n^2. \quad (7)$$

Here, $\sigma_c(V)$ and σ_{ab} are the quasiparticle conductivities perpendicular and along the layers, respectively, and $V = E_z s$ is the voltage between the layers $n+1$ and n. The tunneling conductivity σ_c depends on the voltage in the gapless d-wave superconductor BSCCO (see Ref. 16) and in optimally doped crystals is given by the relation

$$\sigma_c(V) = \sigma_c(0)(1 + bV^2), \quad b \approx 0.004 \text{ meV}^{-2}, \quad (8)$$

where $\sigma_c(0) \approx 1.7\ (\text{k}\Omega\text{cm})^{-1}$ is the conductivity at $V \to 0$.

To account for fluctuation currents $\mathbf{j}_f$ and charges $\rho_{f,n}$, we add to the Lagrangian the term

$$\mathcal{L}_f = -\sum_n \int d\mathbf{r}[(1/c)\mathbf{j}_{f,n}\cdot\mathbf{A}_n - \rho_{f,n}V_n]. \quad (9)$$

In the following, we use the gauge $V_n(\mathbf{r}) = 0$ and omit the last term in $\mathcal{L}_f$.

The power spectrum $P_{qp}(\Omega)$ of quasiparticle fluctuating current density $j_{f,q}$ (in the presence of voltage $V = \hbar\omega_J/2e$) is defined by the expression[11]

$$\langle j_{f,q}(\mathbf{r},t)j_{f,q}(0,0)\rangle = \int_0^\infty d\Omega\, P_{qp}(\Omega)\exp(i\Omega t)\delta(\mathbf{r}),$$

$$P_{qp}(\Omega) = \frac{e}{2\pi}\left[j_{qp}\left(V + \frac{\hbar\Omega}{e}\right)\coth\left(\frac{eV+\hbar\Omega}{2T}\right) + j_{qp}\left(V - \frac{\hbar\Omega}{e}\right)\coth\left(\frac{eV-\hbar\Omega}{2T}\right)\right]. \quad (10)$$

The spectral density of the pair fluctuation currents is

$$P_p(\Omega) = (2e/\pi)j_p(\omega_J/2)\coth(\omega_J/2T) \approx (2e/\pi)J_c\langle\sin\varphi_n\rangle\coth(\omega_J/2T). \quad (11)$$

For low frequencies $\Omega \ll \omega_J$, this results in the correlation function for the total c-axis current density

$$\langle j_{f,c}(0,0,0)j_{f,c}(\mathbf{r},n,\tau)\rangle = \left[\frac{\hbar\omega_J}{\epsilon_0}\frac{\nu_c(V)}{2}\coth\left(\frac{\hbar\omega_J}{4T}\right) + \frac{\hbar\omega_p}{\epsilon_0}\langle\sin\varphi_n\rangle\coth\left(\frac{\hbar\omega_J}{2T}\right)\right]\delta(\mathbf{r})\delta_n\delta(\tau). \quad (12)$$

For the intralayer current, we use the classical expression for the correlation function at $\Omega \ll T$:

$$\langle j_{f,i}(\mathbf{0},0,0)j_{f,j}(\mathbf{r},n,t)\rangle = 2\sigma_{ab}T\delta(\mathbf{r})\delta_n\delta(t)\delta_{ij}. \quad (13)$$

We write down the dimensionless form of the total Lagrangian introducing dimensionless coordinates $u = x/\lambda_J$ and $v = y/\lambda_J$, time $\tau = \omega_p t$, the magnetic field $\mathbf{h} = \mathbf{B}/B_c$, the vector potential $\mathbf{a} = \mathbf{A}/(B_c\lambda_J)$, temperature $\tilde{T} = T/\epsilon_0$, the dissipation parameters $\nu_c = 4\pi\sigma_c/(\omega_p\epsilon_c)$, and $\nu_{ab} = 4\pi\sigma_{ab}/(\omega_p\epsilon_c)$ as well as the intralayer two-component momentum $\mathbf{p} = \lambda_J\mathbf{Q}$. Here, $\omega_p = c/(\lambda_c\sqrt{\epsilon_c})$ is the zero-momentum Josephson plasma frequency. In these variables, the total Lagrangian and the dissipation functions are given by the expressions

$$\frac{\mathcal{L}\{\phi_n,\mathbf{a}\}}{\epsilon_0} = \frac{1}{2}\beta\dot{\varphi}^2 + \sum_n \int du\,dv\left[\frac{1}{2}\dot{\varphi}_n^2 - (1-\cos\varphi_n) - \frac{(\nabla\times\mathbf{a})^2}{2\ell^2} - \frac{1}{2}\mathbf{p}_n^2 + \mathbf{j}_{f,n}\mathbf{a}_n\right], \quad (14)$$

$$\mathcal{R}\{\phi_n,\mathbf{a}\}/\epsilon_0 = \nu_c\sum_n\int du\,dv\,\dot{\varphi}_n^2 + \nu_{ab}\sum_n\int du\,dv\,\dot{\mathbf{p}}_n^2. \quad (15)$$

Here, $\beta = C_s N/C_J$ is the dimensionless parameter of shunt capacitance and $C_J = \epsilon_c L_x L_y/(4\pi s)$ is the capacitance of the intrinsic junction. The Lagrangian and the dissipative function give the equations, for the phases ϕ_n,

$$\frac{d}{dt}\frac{\delta\mathcal{L}}{\delta\dot{\phi}_n} - \frac{\delta\mathcal{L}}{\delta\phi_n} + \frac{\delta\mathcal{R}}{\delta\dot{\phi}_n} = 0. \quad (16)$$

A similar equation for $\mathbf{a}$ gives the following equations for the magnetic field components:

$$(\nabla\times\mathbf{h})_{n,x} = T_{ab}p_{nx} + j_{f,nx}, \quad T_{ab} = 1 + \nu_{ab}\partial/\partial\tau$$
$$(\nabla\times\mathbf{h})_{n,y} = T_{ab}p_{yn} + j_{f,ny}, \quad (17)$$
$$(\nabla\times\mathbf{h})_{n,z} = \sin\varphi_n + \ddot{\varphi}_n + \nu_c\varphi_n + \beta\ddot{\varphi} + j_{f,nz}.$$

By differentiating both sides of Eq. (2) with respect to the coordinates x,y, we get the equation relating the magnetic field with $\mathbf{p}_n$ and φ_n:

$$\nabla_x\varphi_n = p_{x,n+1} - p_{x,n} - \ell^{-2}h_{y,n},$$
$$\nabla_y\varphi_n = p_{y,n+1} - p_{y,n} + \ell^{-2}h_{x,n}. \quad (18)$$

By using the equation $\nabla\cdot[\nabla\times\mathbf{h}] = 0$ and Eqs. (16)–(18), we obtain finally the equation for φ_n:

$$(\nabla_n^2 - \ell^{-2})[\ddot{\varphi}_n + \beta\ddot{\varphi} + \sin\varphi_n + \nu_c\varphi_n - j_{f,z,n}] + \beta\ddot{\varphi} + (1 + \nu_{ab}\partial/\partial\tau)\nabla^2\varphi_n + \nabla\cdot(\mathbf{j}_{f,n+1} - \mathbf{j}_{f,n}) = 0. \quad (19)$$

This equation at $\alpha = \beta = 0$ and without fluctuating currents was obtained in Ref. 17.

The typical parameters of optimally doped BSCCO at low temperatures are $\epsilon_c = 12$, $\gamma = 500$, $\lambda_{ab} = 200$ nm, the critical current $J_c = \phi_0 c/(8\pi^2 s\lambda_c^2) = 1700$ A/cm^2, $\ell = 130$, $\nu_{ab} = 0.2$, and $\nu_c(V = 0) = 0.002$.

First, we will find oscillatory phases neglecting fluctuation currents. For this, we use the perturbation theory with respect to the Josephson coupling for high Josephson frequencies $\omega = \omega_J/\omega_p \gg 1$ and keeping terms not higher than $1/\omega^2$ in the phase difference. At this stage, $\varphi_n = \omega\tau + \phi(u,\tau)$, where $\phi(u,\tau)$ is the part of the phase difference oscillating with the frequency ω. At this stage, radiation occurs at the Josephson frequency without any broadening.

Next, we will find fluctuation contributions to the phase differences by using the perturbation theory with respect to fluctuation currents in the linear approximation in these currents and accounting for the phase $\phi(u,\tau)$ in the Josephson term. At this stage, we present the phase differences as a sum $\varphi_n = \omega\tau + \phi(u,\tau) + \tilde{\theta}_n(\mathbf{r},\tau)$. There is still no broadening of the central radiation line at the Josephson frequency as it is described by $\phi(u,\tau)$. In the final stage, we will find the oscillating part of the phase differences $\tilde{\phi}_n(\mathbf{r},\tau)$, accounting for the fluctuation contribution to the Josephson coupling, by writing in this term $\varphi_n(\tau) = \omega\tau + \tilde{\theta}_n(\mathbf{r},\tau)$. As phases ϕ_n may be changed by any constant term, the fluctuation mode with zero momentum has no gap and, thus, fluctuations induce diffusion of the phase difference. This diffusion results in a decay of the correlation function $\langle\tilde{\theta}_n(\mathbf{r},0)\tilde{\theta}_m(\mathbf{r}',\tau)\rangle$ with time and corresponding broadening of the central line in the oscillating part[12] of $\varphi_n(\tau)$.

III. BOUNDARY CONDITIONS, SOLUTION FOR PHASES, AND THE RADIATION POWER WITHOUT FLUCTUATIONS

The equation for the phase differences [Eq. (19)] is a second-order differential equation with respect to coordinates x,y. To solve it, one needs boundary conditions at the crystal edges. The Maxwell equations in the space outside of the crystal determine the ratio of the magnetic and the electric field at a boundary. From Eqs. (17) and (18), without fluctuation currents, we obtain the expression for the magnetic field via the phase differences

$$\begin{aligned}\left(\nabla_n^2 - \ell^{-2}T_{ab}\right)h_{y,n} + T_{ab}\nabla_u\varphi_n = 0,\\ \left(\nabla_n^2 - \ell^{-2}T_{ab}\right)h_{x,n} - T_{ab}\nabla_v\varphi_n = 0,\end{aligned} \tag{20}$$

while Eq. (4) relates the electric field with the phase difference. Thus, we obtain the relation between space and time derivatives of the phase differences at the crystal edges (see Refs. 8 and 18).

Without fluctuation currents at $\omega \gg 1$ in the geometry shown in Fig. 1, we take the n-independent solution of Eq. (19) with all junctions synchronized due to shunt and radiation (see below). We take also this solution as the y-independent one. In principle, dependence on y in the time-independent part of φ is introduced by the dc magnetic field due to interlayer bias current and in the oscillating part of φ by radiation in the y direction due to momentum conservation.

First, we show that the effect of the dc magnetic field due to bias current is negligible. By using Eqs. (20) and the continuity of B_x and B_y for the time-independent part of the phase difference, we obtain at these boundaries

$$\nabla_{x,y}\varphi_n = \pm(2\pi s/\Phi_0)B_{y,x}. \tag{21}$$

For $L_y \gg L_x$, we estimate $B_y(x = \pm L_x/2, y = \pm L_y/2) \approx \pm 2\pi I/(cL_y)$, while $B_x \lesssim B_y$. Here, $I = \overline{j}_c L_x L_y$ is the total interlayer bias current and $\overline{j}_c$ is the bias current density. Hence, we estimate the time-independent part of the phase difference,

$$\begin{aligned}\varphi(y = L_y/2) - \varphi(y = -L_y/2) &\lesssim 4\pi^2 s j_c L_x L_y/(c\Phi_0)\\ &\lesssim 2\pi\sigma_c\omega_J L_x L_y/c^2.\end{aligned} \tag{22}$$

Here, we used the relation $j_c \approx \sigma_c E_z$ in the resistive state. The estimated phase difference is very small for crystals with L_y smaller thancm and may be neglected. Second, we argue that, when $L_x \ll \lambda_\omega$, radiation in the y direction is weak. So, we may neglect the radiation magnetic field near the boundary $y = \pm L_y/2$ and take the boundary conditions as $\nabla_y\varphi_n = 0$ (see below boundary conditions for $x = \pm L_x/2$ edges).

Next, we find the boundary conditions at $x = \pm L_x/2$ for the oscillating part $\phi(x,\tau)$. To calculate the intrinsic linewidth of radiation, we account only for electromagnetic waves going out of the crystal, discarding any incoming waves including thermal radiation inside the cryostat (boundary conditions in the presence of incoming waves were presented in Ref. 19). In half-spaces $|x| > L_x/2$, the Maxwell equations are

$$\frac{1}{c}\frac{\partial E_z}{\partial\tau} = -\frac{\partial B_y}{\partial x}, \quad \frac{1}{c}\frac{\partial E_x}{\partial\tau} = \frac{\partial B_y}{\partial z}. \tag{23}$$

We take $B_x = B_z = 0$ as the alternating current inside the crystal flows predominantly in the z direction. Taking into account only outgoing waves from the y,z crystal edges, we write

$$B_y(x,z,\tau) \propto \exp(i|k_x|x + ik_z z - i\omega\tau), \tag{24}$$

where $k_x = \sin(\omega)(k_\omega^2 - k_z^2)^{1/2}$ for $k_z^2 < k_\omega^2$ and $k_x = i(k_z^2 - k_\omega^2)^{1/2}$ for $k_z^2 > k_\omega^2$. Here, $k_\omega = \omega/c$. This gives the relation between the Fourier components of the fields at $x = \pm L_x/2$:

$$\begin{aligned}B_y(\omega,k_z) &= \pm\zeta(k_z)E_z(\omega,k_z),\\ \zeta(k_z) &= |k_\omega|\left(k_\omega^2 - k_z^2\right)^{-1/2}, \quad k_z^2 < k_\omega^2\\ \zeta(k_z) &= -ik_\omega\left(k_z^2 - k_\omega^2\right)^{-1/2}, \quad k_z^2 > k_\omega^2.\end{aligned} \tag{25}$$

By inverse Fourier transform with respect to k_z of these equations, we obtain the nonlocal relation between the magnetic and electric fields at the edges $x = \pm L_x/2$. As we assume that the screen material has small surface impedance, we can neglect the electric field at $|z| > L_z/2$. By using Eqs. (4) and (20), we find the boundary conditions connecting h_y with the phase differences at $x = \pm L_x/2$:

$$\begin{aligned}\pm h_y(y,n,\omega) = \frac{is\ell\omega}{2\sqrt{\epsilon_c}}\sum_m \varphi(m,\omega)[|k_\omega|J_0(k_\omega s|n-m|)\\ + ik_\omega N_0(k_\omega|n-m|)],\end{aligned} \tag{26}$$

where $J_0(x)$ and $N_0(x)$ are the Bessel functions and $h_{yn} = \nabla_u\varphi_n$.

For a crystal with a large number of junctions $N \gg \ell$, neglecting finite-size effects along the z axis, we obtain from

Eq. (19) the equation for the n-independent phase difference $\varphi_n(u,\tau)=\varphi(u,\tau)$:

$$\frac{\partial^2}{\partial\tau^2}\left(\varphi+\frac{\beta}{\tilde{L}_x}\int_{-\tilde{L}_x/2}^{\tilde{L}_x/2}\varphi\,du\right)+\nu_c\partial\varphi/\partial\tau+\sin\varphi-\ell^2\nabla_u^2\varphi=0. \tag{27}$$

Here, $\tilde{L}_x=L_x/\lambda_J$. In the limit $\omega\gg 1$, the solution is

$$\varphi(u,\tau)=\omega\tau+\phi(u,\tau) \tag{28}$$

with the oscillating part of the phase difference $\phi(u,\tau)=\mathrm{Im}[\phi(u,\omega)\exp(-i\omega\tau)]\ll 1$. At $k_\omega L_z\ll 1$, Eq. (26) gives the boundary condition for $\phi(u,\omega)$ at $u=\pm\tilde{L}_x/2$:

$$\nabla_u\phi=\pm i\omega\zeta(\omega)\phi(u),$$
$$\zeta(\omega)=\frac{L_z}{2\ell\sqrt{\epsilon_c}}[|k_\omega|-ik_\omega\mathcal{L}_\omega],\ \ \mathcal{L}_\omega=\frac{2}{\pi}\ln\left[\frac{5.03}{|k_\omega|L_z}\right]. \tag{29}$$

The solution of Eq. (27) with these boundary conditions is

$$\phi(u,\tau)=\mathrm{Im}\{[A+B\cos(\bar{k}_\omega u)]e^{-i\omega\tau}\}, \tag{30}$$

where $\bar{k}_\omega=\omega/\ell$. The coefficients in Eq. (30) are

$$A=-\frac{1}{(1+\beta\xi)\omega^2+i\nu_c\omega},\quad a=\epsilon_c L_x/L_z, \tag{31}$$

$$B=\frac{i\zeta}{[(1+\beta\xi)\omega+i\nu_c][\bar{k}_\omega\sin(\bar{k}_\omega\tilde{L}_x/2)+i\zeta\omega\cos(\bar{k}_\omega\tilde{L}_x/2)]}, \tag{32}$$

$$\xi=1+2i\omega\zeta\big/\left(\bar{k}_\omega^2\tilde{L}_x\right)=\{1+a^{-1}[\mathcal{L}_\omega+i\ \mathrm{sign}(\omega)]\}^{-1}. \tag{33}$$

The first term in $\phi(u,\omega)$, Eq. (30), is the amplitude of Josephson oscillations. It drops with β, i.e., the shunt suppresses the radiation. The second term describes the electromagnetic waves propagating inside the crystal. They are generated by the radiation field at the boundaries via the boundary conditions (29), which account for momentum carrying by emitted electromagnetic wave.

For $\langle\sin\varphi_n\rangle$ in Eq. (12), we obtain, in the limit $\mu\omega\tilde{L}_x/\ell\ll 1$,

$$\langle\sin\varphi_n(\tau)\rangle_\tau=\frac{1}{2}\mathrm{Im}\left[A+B\frac{\sin(\bar{k}_\omega\tilde{L}_x/2)}{\bar{k}_\omega\tilde{L}_x/2}\right]$$
$$\approx\frac{1}{2\omega^2}\mathrm{Im}[(\xi^{-1}+\beta)^{-1}]. \tag{34}$$

The Poynting vector P_x at $x=\pm L_x/2$ in terms of the oscillating phase is given by[18]

$$P_x=\pm\frac{\Phi_0^2\omega_J^3}{64\pi^3c^2sN}\sum_{n,m}J_0(k_\omega s|n-m|)|\varphi_\omega(\pm L_x/2)|^2, \tag{35}$$

where the oscillating phase difference is determined by Eq. (30). In the limit $\bar{k}_\omega\tilde{L}_x\ll 1$, we obtain, for the radiation power per crystal unit volume $P_{\mathrm{rad}}(\omega)=P_x/L_x$ going from one side,

$$P_{\mathrm{rad}}(\omega_J)=\left[\Phi_0^2\omega_p^4\epsilon_c/64\pi^3sc^2\omega_J\right]\mathcal{L}(a),$$
$$\mathcal{L}(a)=\frac{a^4}{[a^2+2\beta\mathcal{L}_\omega(a+\beta\mathcal{L}_\omega)][(a+\mathcal{L}_\omega)^2+1]}. \tag{36}$$

For large $\epsilon_c L_x\gg L_z$, we obtain the standard expression for coherent total radiation from one side $\mathcal{P}_{\mathrm{rad}}\propto N^2$, while for small $\epsilon_c L_x\ll L_z$, the total radiation power becomes independent of N, $P_{\mathrm{rad}}\propto L_x^2$.

We see that the power of radiation is determined by the geometrical factor $a=\epsilon_c L_x/L_z$. It depends strongly on L_x and the radiation power vanishes with L_x because the oscillating part of the phase difference ϕ_ω is x dependent due to the boundary conditions (29). These conditions describe negative feedback of radiation on the oscillation part of the phase difference. As $\zeta\propto N$ increases with N and stimulated radiation becomes stronger, the phase $\phi_\omega(u)$ becomes more nonuniform as it takes values proportional to $\pm\zeta$ at $x=\pm L_x/2$. Thus, the amplitude of ϕ_ω drops with N at fixed L_x. As a result, the total radiation power is proportional to N^2 only if L_x also increases with N to accommodate the phase difference $\phi_\omega(L_x/2)-\phi_\omega(-L_x/2)\propto N$ without a significant drop in the oscillating phase amplitude at edges $|\varphi_\omega(\pm L_x/2)|$ in Eq. (35). This effect caused by reaction of the junctions to radiation gives nonstandard dependence of the total radiation power on N at $a\ll 1$ in the regime of coherent radiation.

IV. FLUCTUATION MODES

Fluctuating currents induce the distortions $\tilde{\theta}_n(\mathbf{r},\tau)$. To find them, we write the solution of Eq. (19) as

$$\varphi_n(\mathbf{r},\tau)=\omega\tau+\phi(u,\tau)+\tilde{\theta}_n(\mathbf{r},\tau), \tag{37}$$

and expand in $\tilde{\theta}_n$ keeping only linear terms. The term $\cos[\phi(u,\tau)]\tilde{\theta}_n(\mathbf{r},\tau)\approx\cos(\omega\tau)\tilde{\theta}_n(\mathbf{r},\tau)$ in the linearized equation couples the harmonics of the low-frequency fluctuation mode Ω with the high-frequency harmonics $\Omega\pm\omega$. At $\omega\gg 1$, we can neglect coupling to the higher-frequency harmonics $\Omega\pm m\omega$ with $m>1$ and represent the phase perturbations as

$$\tilde{\theta}_n(\mathbf{r},\tau)\approx\sum_{k,q}\left[\tilde{\theta}_{\mathbf{k}}+\sum_{m=\pm 1}\tilde{\theta}_{\mathbf{k},m}\exp(im\omega\tau)\right]$$
$$\times\cos(k_y y)\cos(qn)\exp(-i\Omega\tau) \tag{38}$$

with $k_y=\pi l/L_y$ and $q=\pi l'/N$. By substituting this presentation into the linearized Eq. (19) and separating the fast and slow parts, we obtain coupled equations describing fluctuation modes with low frequencies Ω and nonzero k_y and q:

$$\left(\Omega^2+i\nu_c\Omega-\overline{C}-G_q^{-2}k_y^2+G_q^{-2}\nabla_u^2\right)\tilde{\theta}_{\mathbf{k}}-(\tilde{\theta}_{\mathbf{k},+}+\tilde{\theta}_{\mathbf{k},-})/2$$
$$=-j_{f,z}(\Omega)+\frac{(e^{iq}-1)[\nabla_u j_{f,x}+ik_y j_{f,y}]_\Omega}{(1-i\nu_{ab}\Omega)\ell^{-2}+2(1-\cos q)}, \tag{39}$$

$$\left[(\Omega\mp\omega)^2+i\nu_c(\Omega\mp\omega)-G_{q,\pm}^{-2}k_y^2+G_{q,\pm}^{-2}\nabla_u^2\right]\tilde{\theta}_{\mathbf{k},\pm}-\tilde{\theta}_{\mathbf{k}}/2$$
$$=-j_{f,z}(\Omega\mp\omega)+\frac{(e^{iq}-1)[\nabla_u j_{f,x}+ik_y j_{f,y}]_{\Omega\mp\omega}}{[1-i\nu_{ab}(\Omega\mp\omega)]\ell^{-2}+2(1-\cos q)}. \tag{40}$$

Here, we denote

$$\overline{C}(u)=\langle\cos[\omega\tau+\phi(u,\tau)]\rangle_\tau\approx\mathrm{Re}[\phi(u,\omega)]/2$$
$$\approx(1/2)\mathrm{Re}[A\cos(k_\omega u)+B], \tag{41}$$
$$G_{q,m}^2=\tilde{q}^2/[1-i(\Omega-m\omega)\nu_{ab}]+\ell^{-2}$$

with $\tilde{q}^2 = 2(1-\cos q)$, and $G_q = G_{q,0}$. By using Eqs. (20) and (25) (in the limit $k_z^2 > k_\omega^2$ due to $k_\omega L_z \ll \pi$) and (29), we get the boundary conditions for slow and fast components at $u = \pm L_x/2\lambda_J$ and $q \gg \pi/N$:

$$\nabla_u \tilde{\theta}_{\mathbf{k}} = \pm\kappa_0 \tilde{\theta}_{\mathbf{k}}, \quad \kappa_0 = G_q^2 \Omega^2/(\epsilon_c q\gamma), \tag{42}$$

$$\nabla_u \tilde{\theta}_{\mathbf{k},m} = \pm\kappa_m \tilde{\theta}_{\mathbf{k},m}, \quad \kappa_m \approx \frac{(\Omega - m\omega)^2 G_{q,m}^2}{\epsilon_c q\gamma}. \tag{43}$$

To find $\tilde{\theta}_{\mathbf{k}}(u)$, we need to solve Eq. (40) for $\tilde{\theta}_{\mathbf{k},\pm}(u)$ and put the solution into Eq. (39). In the right-hand side of Eq. (40), we neglect the fluctuation currents because their contribution is smaller by the factor $1/\omega^2$ in comparison with the low-frequency currents presented in Eq. (39). Due to the condition $|\Omega| \ll \omega$, one can neglect also Ω in Eq. (40). We also assume $\nu_c \ll 1 \ll \omega$ and neglect dissipation where it is possible. As $\tilde{\theta}_{\mathrm{k}}(u)$ varies at the typical scale $\sim 1/(G_q\Omega) \gg \tilde{L}_x$, it can be treated as a constant in equations for $\tilde{\theta}_{\mathbf{k},\pm}(u)$. By substituting the solution for $\tilde{\theta}_{\mathbf{k},\pm}(u)$ into Eq. (39), we obtain the Mathieu equation for the slow-varying component $\tilde{\theta}_{\mathbf{k}}(u)$ with nonzero right-hand side:

$$\left[\Omega^2 + i\nu_c\Omega - G_q^{-2}k_y^2 - \Lambda - V(u) + G_q^{-2}\nabla_u^2\right]\tilde{\theta}_{\mathbf{k}} = -j_{f,z}(\Omega) + \frac{(e^{iq}-1)[\nabla_u j_{f,x} + ik_y j_{f,y}]_\Omega}{(1-i\nu_{ab}\Omega)\ell^{-2} + (1-\cos q)}, \tag{44}$$

$$\Lambda = \frac{1}{2(\omega^2+\nu_c^2)} - \mathrm{Re}\left[\frac{1}{2[(1+\beta\xi)\omega^2 + i\omega\nu_c]}\right], \tag{45}$$

with the potential $V(u) = V_1(u) + V_2(u)$:

$$V_1(u) = \frac{1}{2\omega^2}\mathrm{Re}\left[\frac{i\zeta\omega\cos(\bar{k}_\omega u)}{(1+\beta\xi)[\bar{k}_\omega \sin(\bar{k}_\omega \tilde{L}_x/2) + i\zeta\omega\cos(\bar{k}_\omega \tilde{L}_x/2)]}\right],$$

$$V_2(u) = \frac{1}{2\omega^2}\mathrm{Re}\left[\frac{\kappa_+\cos(p_+ u)}{(1+\beta\xi)[p_+\sin(p_+\tilde{L}_x/2) + \kappa_+\cos(p_+\tilde{L}_x/2)]}\right].$$

Here, $p_+ = \omega G_{q+}$ and $\kappa_+ \approx [(\Omega-\omega)^2 G_{q,+}^2]/(\epsilon_c q\gamma)$. In the lowest order in $\bar{k}_\omega \tilde{L}_x = \omega\tilde{L}_x/\ell \ll 1$, the part $V_1(u)$ reduces to a constant

$$V_1(u) \approx \mathcal{K}_\omega/(2\omega^2), \tag{46}$$

$$\mathcal{K}_\omega = \mathrm{Re}\left[\frac{1}{1+\beta\xi}\left(\beta + \frac{\mathcal{L}_\omega + i}{a + \mathcal{L}_\omega + i}\right)\right]. \tag{47}$$

For eigenvalues of fluctuation modes, by treating the coordinate-dependent part of $\tilde{\theta}_{\mathbf{k}}(u)$ as a small perturbation, we find the expression for the dispersion $\Omega(\mathbf{k},q)$:

$$\Omega^2(q,\mathbf{k}) + i\Omega\Gamma(q,\mathbf{k}) = \epsilon_g^2 + \frac{k_x^2 + k_y^2}{\ell^{-2} + 2(1-\cos q)}, \tag{48}$$

$$\Gamma(q,\mathbf{k}) = \nu_c + \frac{2\nu_{ab}\mathbf{k}^2(1-\cos q)}{[\ell^{-2} + 2(1-\cos q)]^2}, \tag{49}$$

$$\epsilon_g^2 = \frac{1}{2\omega^2}\left(\mathcal{K}_\omega - \mathrm{Re}\left[\frac{W_2(q)}{1+\beta\xi}\right]\right), \quad W_2(q) = \frac{2}{p_+\tilde{L}_x[p_+/\kappa_+ + \cot(p_+\tilde{L}_x/2)]}. \tag{50}$$

Here, $k_x \approx \pi p/L_x$, where p is an integer. The fluctuations with nonzero momenta $\mathbf{k}$ or q have the gap ϵ_g in their spectrum. The first term, $\mathcal{K}_\omega$, in curly brackets for the gap squared [Eq. (50)] describes the effect of the shunt and the radiation. They both introduce the gap of the order ω^{-2} in the spectrum of fluctuation modes. As β increases from 0 to the values $\beta \gg 1$, the gap due to the shunt increases, while that due to the radiation drops. The last term W_2 originates from the boundary conditions (43) and it describes the effect of modes $\tilde{\theta}_{q\pm}$ induced inside the crystal due to the radiation (excitated Fiske modes). This term leads to the instability for small $\mathbf{k}$ and q in the limit of zero dissipation and in the absence of other stabilizing terms, but it is strongly suppressed by the in-plane dissipation. It is the same destructive effect of the radiation that results in the drop of the radiation power when N increases at fixed L_x. However, even without shunt, the radiation term $\mathcal{K}_\omega$ prevails, $\mathcal{K}_\omega > W_2(q)$ for nonzero q, and the net result of the radiation is the stabilization of uniform Josephson oscillations by suppressing excitation of nonuniform Fiske modes.

Solving Eq. (44) with $\Omega(\mathbf{k},q)$ and $\Gamma(\mathbf{k},q)$ presented above and with the fluctuating quasiparticle currents in the right-hand side, we find the amplitudes of slow fluctuating mode with nonzero momenta

$$\tilde{\theta}_{\mathbf{k}} \approx [\Omega^2 - \Omega^2(q,\mathbf{k}) + i\Omega\Gamma]^{-1}\mathcal{J}(\mathbf{k},q,\Omega), \tag{51}$$

$$\mathcal{J}(\mathbf{k},q,\Omega) = \left[-j_{f,z}(q,\mathbf{k},\Omega) + \frac{i(e^{iq}-1)\mathbf{k}\cdot\mathbf{j}_f(q,\mathbf{k},\Omega)}{(1-i\nu_{ab}\Omega)\ell^{-2} + (1-\cos q)}\right]. \tag{52}$$

The homogeneous mode requires special consideration. For $q = k_y = 0$, we obtain

$$[(1+\beta)\Omega^2 + i\nu_c\Omega - \overline{C}]\tilde{\theta}(0,\Omega) + \ell^2\nabla_u^2\tilde{\theta}(0,\Omega) - (1/2)[\tilde{\theta}_+(0,\omega+\Omega) + \tilde{\theta}_-(0,\omega-\Omega)] = -j_{f,z}(0,u,\Omega), \tag{53}$$

$$[(1+\beta)(\Omega\mp\omega)^2 + i\nu_c(\Omega\mp\omega)]\tilde{\theta}_\pm(0,\omega\pm\Omega) + \ell^2\nabla_u^2\tilde{\theta}_\pm(0,\omega\mp\Omega) - \tilde{\theta}(0,\Omega)/2 = -j_{f,z}(0,u,\Omega\pm\omega). \tag{54}$$

These equations differ from those for nonzero momenta by the factor $(1+\beta)$ in front of Ω^2 and $(\Omega\pm\omega)^2$. The boundary conditions at $u = \pm L_x/2$ are also different:

$$\nabla_u\tilde{\theta}_\pm(0,u,\omega\pm\Omega) = \pm i(\omega\pm\Omega)\zeta(\omega\pm\Omega)\tilde{\theta}_\pm(0,u,\omega\pm\Omega), \tag{55}$$

while for the slow harmonic, we take, at $u = \pm L_x/2$,

$$\nabla_u\tilde{\theta}(0,\Omega) = \pm i\Omega\zeta(\Omega). \tag{56}$$

The right-hand side is $\propto \Omega^2$ and we set it to zero at low Ω. Later, we will see that terms of order Ω^2 are irrelevant there.

First, we show that broadening of the central line $\Omega = 0$ is determined by the mode uniform in the x direction. By solving Eq. (53) for a given j_z and $\tilde{\theta}_\pm$ with the boundary conditions (56), we obtain

$$\tilde{\theta}(u) = \frac{1}{\tilde{L}_x}\sum_{p_n}\frac{\cos(p_n u)[-2j_{f,z}(0,n,\Omega)+\tilde{\theta}_+(0,n,\omega+\Omega)+\tilde{\theta}_-(0,n,\omega-\Omega)]}{(1+\beta)\Omega^2+i\Omega(\nu_c+\nu_r)-\ell^2p_n^2}, \tag{57}$$

where we introduced the notations

$$A(0,n,\Omega) = \int du\, A(0,u,\Omega)\cos(p_n u), \quad p_n = 2\pi n/\tilde{L}_x.$$

The modes with nonzero n have dimensionless frequencies (in units of ω_p) $\Omega_n = (2\pi n\ell/\tilde{L}_x)^2$ much larger than unity for $L_x \leqslant 10\ \mu$m and, thus, we need to account for only the mode with $n = 0$. By averaging Eq. (54) over u and accounting for the boundary conditions (55), we obtain

$$\langle\tilde{\theta}_\pm(0,\Omega)\rangle = \frac{1}{2}\frac{\langle\tilde{\theta}(0,\Omega)\rangle}{(1+\beta)(\Omega\mp\omega)^2+i\nu_c(\Omega\mp\omega)+(2i\ell^2/\tilde{L}_x)(\Omega\mp\omega)\zeta(\Omega\mp\omega)}. \tag{58}$$

By averaging Eq. (53) with the boundary conditions (56) and setting $\langle\tilde{\theta}_\pm(0,\Omega)\rangle$, we obtain the equation

$$(1+\beta)(\Omega^2+i\nu_c\Omega-\overline{C})\langle\tilde{\theta}(0,\Omega)\rangle - \frac{1}{4}\sum_{m=\pm}(2i\ell^2/\tilde{L}_x)\zeta(\Omega-m\omega)\langle\tilde{\theta}_m(0,\Omega)\rangle = -\langle j_{f,z}(0,u,\Omega)\rangle. \tag{59}$$

It gives the equation for $\langle\tilde{\theta}(0,\Omega)\rangle$:

$$[(1+\beta)\Omega^2+i\nu_c\Omega-\overline{C}]\langle\tilde{\theta}(0,\Omega)\rangle - (1/2)\sum_{\delta=\pm1}\frac{\tilde{\theta}(0,\Omega)/2-\langle j_{f,z}(0,u,\Omega-\delta\omega)\rangle}{(1+\beta)(\Omega-\delta\omega)^2+i\nu_c(\Omega-\delta\omega)+(2i\ell^2/\tilde{L}_x)\zeta(\Omega-\delta\omega)} = 0. \tag{60}$$

In the term with the summation over δ, we make expansion in Ω and obtain the equation for $\tilde{\theta}(0,\Omega)$ with the term accounting for radiation:

$$[(1+\beta)\Omega^2+i(\nu_c+\nu_r)\Omega]\tilde{\theta}(0,0,\Omega) = -j_{f,z}(0,0,\Omega), \tag{61}$$

$$\nu_r = [(1+\beta)a\omega^3]^{-1}\mathcal{L}_\omega. \tag{62}$$

The radiation term ν_r reaches maximum of the order ν_c at $a = (1+\mathcal{L}_\omega)^{1/2}$ because, at this value, the radiation power per unit volume of the crystal is maximum. It is small in the limiit $a \gg 1$ when $P_{\rm rad} \propto N^2$, i.e., in the regime of strongly stimulated radiation. It becomes small in the opposite limit as well because there the radiation power is small.

Thus, we need to account for zero mode $k_y = q = n = 0$,

$$\tilde{\theta}(0,0,\Omega) = -\frac{j_{f,z}(0,0,\Omega)}{\Omega[(1+\beta)\Omega+i(\nu_c+\nu_r)]}. \tag{63}$$

This mode is gapless because the overall phase of the superconducting order parameter is not fixed. It is the diffusion of this slow mode due to fluctuations that leads to the line broadening. Now we see that terms omitted in the right-hand side of Eq. (56) affect insignificantly the low-frequency behavior of the diffusion mode.

V. RADIATION LINEWIDTH

Now we find the oscillating part of the phase difference $\tilde{\phi}_n(\mathbf{r},\tau)$ by solving Eq. (19) for $\omega \gg 1$ accounting for the fluctuation contribution to the phase difference, i.e., taking

$$\varphi_n(\mathbf{r},\tau) = \omega\tau + \tilde{\theta}_n(\mathbf{r},\tau) \tag{64}$$

in the Josephson term $\sin[\varphi_n(\mathbf{r},\tau)]$, but omitting the term $\tilde{\phi}_n(\mathbf{r},\tau) \sim \omega^{-2}$ there. We obtain

$$\tilde{\phi}(\mathbf{k},q,\Omega) = \Omega^{-2}\{\sin[\omega\tau+\tilde{\theta}_n(\mathbf{r},\tau)]\}_{\mathbf{k},q,\Omega},$$
$$\{\sin[\omega\tau+\tilde{\theta}_n(\mathbf{r},\tau)]\}_{\mathbf{k},q,\Omega} = \sum_n\int d\mathbf{r}\,d\tau\, e^{-i(\mathbf{kr}+qn+i\Omega\tau)}\sin[\omega\tau+\tilde{\theta}_n(\mathbf{r},\tau)]. \tag{65}$$

The correlation function that determines the line broadening is

$$F(\mathbf{r},n,\tau) = \langle\tilde{\phi}_n(\mathbf{r},\tau)\tilde{\phi}_0(0,0)\rangle = \sum_{\mathbf{k},q,\mathbf{k}',q'} e^{i(\mathbf{kr}+qn+\Omega\tau)}\int d\Omega\int d\Omega'(\Omega\Omega')^{-2} \times\langle\{\sin[\omega\tau+\tilde{\theta}_n(\mathbf{r},\tau)]\}_{\mathbf{k},q,\Omega}\{\sin[\omega\tau+\tilde{\theta}_n(\mathbf{r},\tau)]\}_{\mathbf{k}',q',\Omega'}\rangle. \tag{66}$$

By presenting the product of sines as a sum and difference of cosines, dropping the sum term, and using the relation for Gaussian random variables

$$\langle\cos[\tilde{\phi}_n(\mathbf{r},\tau)-\tilde{\phi}_0(0,0)]\rangle = \exp\{-\langle[\tilde{\phi}_n(\mathbf{r},\tau)-\tilde{\phi}_0(0,0)]^2/2\rangle\}, \tag{67}$$

we obtain

$$F(n,\mathbf{r},\Omega) = \int \Omega^{-4}d\tau\cos(\omega_J\tau)e^{i\Omega\tau}\exp[-K(\mathbf{r},n,\tau)], \tag{68}$$

$$K(\mathbf{r},n,\tau) = (1/2)\langle[\tilde{\phi}_n(\mathbf{r},\tau)-\tilde{\phi}_0(0,0)]^2\rangle = \sum_{\mathbf{k},q}\int d\Omega\frac{1-\cos(\mathbf{kr}+qn+\Omega\tau)}{2\pi\Omega^4}\langle\mathcal{J}^2(\mathbf{k},q,\Omega)\rangle. \tag{69}$$

Here,

$$\begin{aligned}\langle \mathcal{J}^2(\mathbf{k},q)\rangle \equiv \mathcal{T}(\mathbf{k},q) &= \langle j_{f,z}^2(\mathbf{k},q)\rangle \\ &+ \frac{2\mathbf{k}^2(1-\cos q)\nu_{ab}}{(1-\cos q+\ell^{-2})^2}\langle \mathbf{j}_f^2(\mathbf{k},q)\rangle \\ &= \frac{\hbar\omega_J}{\epsilon_0}\left\{\frac{1}{4}\nu_c(V)\coth\left(\frac{\hbar\omega_J}{4T}\right)\right. \\ &\left.-\frac{1}{2\omega^3}\coth\left(\frac{\hbar\omega_J}{2T}\right)\mathrm{Im}[(\xi^{-1}+\beta)^{-1}]\right\} \\ &+ \frac{4\nu_{ab}\tilde{T}\mathbf{k}^2(1-\cos q)}{(1-\cos q+\ell^{-2})^2}. \end{aligned} \quad (70)$$

From Eq. (68), we see that $\mathcal{F}(\mathbf{k},q,\Omega)$ is peaked at $\Omega=\omega_J$, while the factor $\exp[-K(\mathbf{r},n,\tau)]$ results in the broadening and in the suppression of this peak. In the correlation function $F(\mathbf{r},n,\Omega)$, we approximate $\Omega^{-4}\approx\omega_J^{-4}$. Hence,

$$F(\mathbf{r},n,\Omega)=\omega_J^{-4}\int d\tau\cos(\omega_J\tau)\cos(\Omega\tau)\exp[-K(\mathbf{r},n,\tau)]. \quad (71)$$

In fact, $\exp[-K(\mathbf{r},n\tau)]$ is the Debye-Waller factor describing suppression of coherent Josephson oscillations by fluctuation modes. To derive this factor, we first integrate over Ω separating the term corresponding to $\mathbf{k}=0$, $q=0$, and the term $n=0$:

$$\begin{aligned} K(\mathbf{r},n,\tau) &= \frac{1}{2\pi(1+\beta)^2\tilde{L}_x\tilde{L}_yN} \\ &\times\left[\int d\Omega\frac{\mathcal{T}(\mathbf{k}=0,q=0)[1-\cos(\Omega\tau)]}{\Omega^2(\Omega^2+\nu^2)}\right. \\ &\left.+\sum_{\mathbf{k},q\neq 0}\int d\Omega\frac{\mathcal{T}(\mathbf{k},q)[1-\cos(\Omega\tau)\cos(\mathbf{kr})\cos(qn)]}{|\Omega^2-\Omega^2(\mathbf{k},q)+i\Omega\Gamma(\mathbf{k},q)|^2}\right] \end{aligned} \quad (72)$$

$$\begin{aligned} &= \frac{1}{2(1+\beta)^2\tilde{L}_x\tilde{L}_yN}\left\{\mathcal{T}(0)\left[\frac{\tau}{\nu^2}+\frac{1-e^{-\nu\tau}}{\nu^3}\right]\right. \\ &\left.+\sum_{\mathbf{k},q\neq 0}\frac{\mathcal{T}(\mathbf{k},q)\exp[-\Gamma(\mathbf{k},q)\tau/2]\cos(\mathbf{kr})\cos(qn)}{\Omega^2(\mathbf{k},q)\Gamma(\mathbf{k},q)}\right\}. \end{aligned} \quad (73)$$

Here, $\nu=(\nu_c+\nu_r)/(1+\beta)$. In the presence of the gap in the fluctuation spectrum, the term with $\cos(\mathbf{kr})\cos(qn)$ at nonzero $\mathbf{k}$ and q in in Eq. (73) vanishes as $\exp(-\epsilon_g y/\lambda_J)$ and $\exp(-\epsilon_g n)$ in the limit of large y and n, respectively. The remaining terms

$$\begin{aligned} K(L_y,N,\tau) &= \frac{1}{2\tilde{L}_x\tilde{L}_yN}\left[\frac{\mathcal{T}(0)}{(1+\beta)^2}\left(\frac{\tau}{\nu^2}+\frac{[1-e^{-\nu\tau}]}{\nu^3}\right)\right. \\ &\left.+\sum_{\mathbf{k},q\neq 0}\frac{\mathcal{T}(\mathbf{k},q)}{\Omega^2(\mathbf{k},q)\Gamma(\mathbf{k},q)}\right] \end{aligned} \quad (74)$$

describe broadening and suppression of coherent radiation from the whole crystal when $\tilde{L}_y/\lambda_J, N \gg \omega$. The broadening due to the first term with $\mathcal{T}(0)$ gives the Lorentzian radiation linewidth

$$\Delta\Omega_L=\frac{s\lambda_J^2\mathcal{T}(0)}{2L_xL_yL_z(\nu_c+\nu_r)^2}\quad\text{for}\quad\frac{s\lambda_J^2\mathcal{T}(0)}{2L_xL_yL_z(\nu_c+\nu_r)^2}\ll 1, \quad (75)$$

while the line is Gaussian with the width

$$\begin{aligned}\Delta\Omega_G &= \left[\frac{s\lambda_J^2\mathcal{T}(0)}{2(1+\beta)L_xL_yL_z(\nu_c+\nu_r)}\right]^{1/2} \\ &\text{for}\quad \frac{s\lambda_J^2\mathcal{T}(0)}{2L_xL_yL_z(\nu_c+\nu_r)^2}\gg 1. \end{aligned} \quad (76)$$

For $\mathcal{T}(0)$, we derive

$$\mathcal{T}(0)=\frac{\hbar\omega_J\nu_c}{2\epsilon_0}\left[1+\frac{1}{a\omega^3\nu_c(1+a\mathcal{L}_\omega)^2}\right]. \quad (77)$$

The relative Lorentzian linewidth $r=\Delta\Omega_L/\omega_J$ is

$$r=\frac{e^2}{\hbar c}\frac{4\pi s^2\lambda_c\nu_c}{\sqrt{\epsilon_c}(\nu_c+\nu_r)^2L_xL_yL_z}\left[1+\frac{1}{a\omega^3\nu_c(1+a\mathcal{L}_\omega)^2}\right]. \quad (78)$$

Note that the radiation term ν_r diminishes the linewidth because it suppresses the amplitude of the fluctuation modes. In the crystal with $L_x=8$ μm, $L_y=300$ μm, and $L_z=80$ μm, we predict the Lorentzian lineshape with the relative width 10^{-8} at the frequency 1 THz.

Let us now estimate the Debye-Waller factor $\exp[-K(0,L_y,N,0)]$. We obtain

$$K(0,L_y,N,0)=\sum_{\mathbf{k},q\neq 0}\frac{\mathcal{T}(\mathbf{k},q)}{\Omega^2(\mathbf{k},q)\Gamma(\mathbf{k},q)} \quad (79)$$

$$\begin{aligned} &= \frac{\mathcal{T}(0)}{8\pi\nu_c(d-1)}\ln d+\frac{\tilde{T}}{\pi}\left[\ln\left(1+\frac{\lambda_c\nu_{ab}}{\xi_0\nu_c}\right)\right. \\ &\left.+\frac{\nu_{ab}}{\nu_c(1-d)}\ln d\right],\quad d=\epsilon_g^2\nu_{ab}/\nu_c. \end{aligned} \quad (80)$$

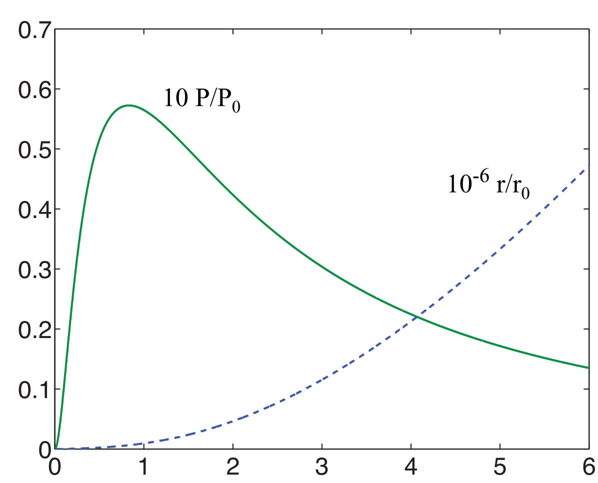

FIG. 2. (Color online) Dependence of the relative linewidth $r(a)$ and the radiated power $P(a)$ on the geometrical factor $a=\epsilon_cL_x/L_z$. The parameter $r_0=(e^2/\hbar c)(4\pi s^2\lambda_c\nu_c/\epsilon_c^{3/2}L_x^2L_y)$ and $P_0=\phi_0^2\omega_p^4L_x^2L_y/[64\pi^4(1+\beta)c^2s^2\epsilon_c^2\omega_J]$.

Putting in numbers, we obtain $K(0,L_y,N,0) \approx 0.1$, i.e., suppression of the radiation power by fluctuations is weak due to the gap for fluctuations with nonzero $\mathbf{k},q$.

The radiation power from one crystal side in the frequency interval $(\omega_J + \Omega, \omega_J + \Omega + d\Omega)$ near the Josephson frequency ω_J is given by the expression

$$P_{\rm rad}(\omega_J + \Omega)d\Omega = \frac{\phi_0^2 \omega_p^4 N^2 L_y \mathcal{L}(a)}{64\pi^4(1+\beta)c^2\omega_J} \frac{\Delta\Omega_L}{\Omega^2 + \Delta\Omega_L^2} d\Omega \quad (81)$$

in the case of the Lorentzian lineshape. The dependence of $r(a)$ and $P_{\rm rad}(a)$ is shown in Fig. 2.

VI. CONCLUSIONS

Both the super-radiation, when many junctions in the crystal are synchronized, and the shunt capacitance introduce a gap in the spectrum of the fluctuation modes with nonzero momenta and, in this way, they stabilize coherent Josephson oscillations in the entire crystal. The gap ϵ_g, given by Eq. (50), is formatted because each junction is coupled with all other junctions in the stack via the field in the shunt capacitance and via the radiation field. For a shunt to be effective, the condition of comparable NC_s and C_J should to be fulfilled, i.e., the parameter $\beta = 2\pi C_s N/C_J$ should not be very small. Here, C_J is the capacitance of a single intrinsic junction. For a crystal with $L_x \times L_y = 4 \times 300\ \mu\text{m}^2$, we get $C_J = 60$ cm ($\approx$0.06 pF) and the condition $\beta \sim 1$ is easy to satisfy. A shunt capacitance of this order of magnitude decreases the time of establishment of synchronized oscillations after a dc current is switched on, while at this stage the radiation is still weak and can not effectively synchronize oscillations in different junctions. After reaching the super-radiation regime in a crystal with many junctions (10^4–10^5), a shunt capacitance becomes unimportant for stabilization and may be switched off or diminished significantly as it decreases the radiation power.

The gap in the spectrum of the fluctuation modes with nonzero momenta keeps the relative radiation linewidth very low. The linewidth determined by the phase diffusion is inversely proportional to the crystal volume, similar to the situation in lasers. For BSCCO at 4 K and the radiation frequency 1 THz, we obtain $r \sim 10^{-8}$ in the crystal with the dimensions $8 \times 300 \times 80\ \mu\text{m}^3$. One can decrease r further by increasing the crystal length L_y. One needs to keep $L_z \leqslant \lambda_\omega/2$ and, thus, increase of L_x beyond L_z/ϵ_c is not useful as it results in bigger heat production without significant change of the radiation power.

We note the characteristic property of radiation from IJJ in contrast to usual radiating systems. First, the radiation affects strongly the amplitude of the Josephson oscillations inside the crystal because it results in a nonuniform oscillating part of the phase difference in the direction of radiation [Eq. (29)]. This backward effect of radiation is a consequence of the momentum conservation as the radiation carries the momentum. As the number of junctions N increases, stimulated radiation also increases, resulting in the drop of the amplitude of the Josephson oscillations if the crystal thickness L_x is fixed. However, if one increases the crystal thickness L_x simultaneously with N to accommodate radiation-induced nonuniformity, amplitude would not drop. The backward effect of radiation results in the dependence of the total radiation power on the geometric factor $a = \epsilon_c L_x/L_z$ and the total radiation power is proportional to N^2 only if $a \gtrsim 1$. In this case, the effect of the radiation on the Josephson oscillations becomes insignificant. Thus, when a stack of IJJ radiates directly into the space outside of the crystal, the source of radiation, i.e., the Josephson oscillations, is affected by the radiation. In usual radiating systems, an antenna is loaded by the ac current source with given ac current or ac voltage and, thus, the radiating field depends on the antenna geometry and the surrounding space. In a IJJ stack radiating directly outside of the crystal, such a separation of the source and the radiating system (antenna) makes no sense. Hence, the source (amplitude of Josephson oscillations) and the radiation should be found self-consistently. Only when the radiation is weak can one find the electric field at the crystal edges and then use the Huigens principle to find the radiation field.[20]

ACKNOWLEDGMENTS

The work of I.M. and L.N.B. was carried out under the auspices of the National Nuclear Security Administration of the U. S. Department of Energy at Los Alamos National Laboratory under Contract No. DE-AC52-06NA25396 and supported by the LANL/LDRD Program. I.M. and L.B. were supported in part by the National Science Foundation under Grant No. PHY05-51164. G.B.H. acknowledges Professor J. Driscoll of Trinity College, Cambridge, for supporting this research. The authors thank A. E. Koshelev for helpful discussions.

[1] D. N. Langenberg, D. J. Scalapino, B. N. Taylor, and R. E. Eck, Phys. Rev. Lett. **15**, 294 (1965); I. K. Yanson, V. M. Svistunov, and I. M. Dmitrenko, Zh. Eksp. Teor. Fiz. **48**, 976 (1965) [Sov. Phys. JETP **21**, 650 (1965)].

[2] A. K. Jain, K. K. Likharev, J. E. Lukens, and J. E. Sauvageau, Phys. Rep. **109**, 309 (1984).

[3] J. Lukens, *Superconducting Devices* (Plenum, New York, 1990), p. 135; P. Barbara, A. B. Cawthorne, S. V. Shitov, and C. J. Lobb, Phys. Rev. Lett. **82**, 1963 (1999).

[4] S. Y. Han, B. Bi, W. Wanxing, and J. E. Lukens, Appl. Phys. Lett. **64**, 1424 (1994).

[5] F. Song, F. Müller, R. Behr, and A. M. Klushin, Appl. Phys. Lett. **95**, 172501 (2009).

[6] T. Koyama and M. Tachiki, Solid State Commun. **96**, 367 (1995); G. Hechtfischer, W. Walkenhorst, G. Kunkel, K. Schlenga, R. Kleiner, P. Muller, and H. L. Johnson, IEEE Trans. Appl. Supercond. **7**, 2723 (1997); Yu. I. Latyshev, M. B. Gaifullin, M. Machida, and Yu. Matsuda, Phys. Rev. Lett. **87**, 247007 (2001); M. Tachiki, M. Iizuka, K. Minami, S. Tejima, and H. Nakamura, Phys. Rev. B **71**, 134515 (2005).

[7] L. Ozyuzer, A. E. Koshelev, C. Kurter, N. Gopalsami, Q. Li, M. Tachiki, K. Kadowaki, T. Yamamoto, H. Minami, H. Yamaguchi,

T. Tachiki, K. E. Gray, W.-K. Kwok, and U. Welp, Science **318**, 1291 (2007); K. Kadowaki, H. Yamaguchi, K. Kawamata, T. Yamamoto, H. Minami, I. Kakeya, U. Welp, L. Ozyuzer, A. Koshelev, C. Kurter, K. E. Gray, and W.-K. Kwok, Phys. C (Amsterdam) **468**, 634 (2008); K. E. Gray, A. E. Koshelev, C. Kurter, K. Kadowaki, T. Yamamoto, H. Minami, H. Yamaguchi, M. Tachiki, W.-K. Kwok, and U. Welp, IEEE Trans. Appl. Supercond. **19**, 886 (2009).

[8] L. N. Bulaevskii and A. E. Koshelev, Phys. Rev. Lett. **99**, 057002 (2007).

[9] A. A. Chernikov and G. Schmidt, Phys. Rev. E **52**, 3415 (1995).

[10] I. Martin, G. Hálash, L. N. Bulaevskii, and A. E. Koshelev, Appl. Phys. Lett. **108**, 033908 (2010).

[11] A. J. Dahm, A. Denenstein, D. N. Langerberger, W. H. Parker, D. Rogovin, and D. J. Scalapino, Phys. Rev. Lett. **22**, 1416 (1969).

[12] A. Varlamov and A. Larkin, *Theory of Fluctuations in Superconductors* (Oxford University Press, New York, 2009).

[13] L. Mandel and E. Wolf, *Optical Coherence and Quantum Optics* (Cambridge University Press, Cambridge, UK, 1995), p. 960.

[14] L. N. Bulaevskii, D. Dominguez, M. P. Maley, A. R. Bishop, and B. I. Ivlev, Phys. Rev. B **53**, 14601 (1996).

[15] T. Koyama and M. Tachiki, Phys. Rev. B **54**, 16183 (1996).

[16] Yu. I. Latyshev, T. Yamashita, L. N. Bulaevskii, M. J. Graf, A. V. Balatsky, and M. P. Maley, Phys. Rev. Lett. **82**, 5345 (1999).

[17] L. N. Bulaevskii, M. Zamora, D. Baerisvyl, H. Beck, and J. R. Clem,Phys. Rev. B **50**, 12831 (1994).

[18] L. N. Bulaevskii and A. E. Koshelev, J. Supercond. Novel Magn. **19**, 349 (2006).

[19] L. N. Bulaevskii, A. E. Koshelev, and M. Tachiki, Phys. Rev. B **78**, 224519 (2008).

[20] R. S. Elliott, *Antenna Theory and Design* (Wiley, New York, 1981).